Dyhydropyridines (DHPs) is a major class of L-type calcium channel (LCC) ligands, which have boat-like six-membered ring with NH-group at the stern, aromatic moiety at the bow, and various substituents at the port and starboard sides. DHPs demonstrate antagonistic or agonistic action, which was previously explained as stabilization or destabilization, respectively, of the closed-gate state by the hydrophilic or hydrophobic port-side substituent. Here we used Monte Carlo energy-minimizations to dock various DHPs in the open-LCC model (Tikhonov & Zhorov, 2008). The calculations suggest a novel structural model in which agonistic and antagonistic actions are determined by different parts of the DHP molecule and have different molecular mechanisms. In our model, DHP polar moieties at the stern, bow, and starboard form H-bonds with side chains of Tyr_IVS6, Tyr_IIIS6, and Gln_IIIS5, respectively. The aromatic moiety at the bow binds to Phe_IIIP. We propose that these contacts with the well-known DHP-sensing residues stabilize the channel's open-gate conformation. Since these contacts are common for various DHPs, our model explains why both agonist and antagonists increase probability of the long-lasting channel openings and why even partial disruption of the contacts eliminates the agonistic action. In our model, the port-side is exposed to the permeation pathway and approaches the selectivity filter. Hydrophobic ports-side group of antagonists may induce long-lasting channel closings by destabilizing calcium coordination with the selectivity-filter glutamates in domains III and IV. In contrast, agonists, which have either hydrophilic or no substituent at the port-side, lack this destabilizing effect. Our model explains action of DHPs with diverse substituents. Thus, long substituents at the port-side are readily accommodated in the pore. Long substituents at the starboard-side protrude in the III/IV domain interface, explaining activity of DHPs linked to a permanently charged group. Supported by CIHR.

945-Pos Board B824

Reinterpretation of SCAM Data in View of Kv1.2-based Models of MTSET-Substituted CaV2.1 Channels

Iva Bruhova, Boris S. Zhorov.
McMaster University, Hamilton, ON, Canada.

Molecular modeling of calcium channels, which are important drug targets, relies on sequence alignments with potassium channels. Huber et al. (2000) and Zhorov et al. (2001) proposed alignments for outer and inner helices, respectively. Zhen et al. (2005) attempted to identify pore-lining residues in CaV2.1 channel using the substituted-cysteine accessibility method (SCAM) and interpreted their data as inconsistent with known sequence alignments. Indeed, the inner-helix residues in positions *i15*, *i18*, *i19*, and *i22* face the Kv1.2 pore. In agreement with this, 2-(trimethylammonium)ethyl methanethiosulfonate (MTSET) applications to CaV2.1 with engineered cysteines in positions *2i18* (domain 2, inner-helix position 18)*, 4i18,* and positions *i15* and *i19* of all four domains decreased current. However, CaV2.1 with cysteine substitutions in positions *1i18*, *3i18* and position *i22* of all four domains were not blocked by MTSET. Furthermore, despite the outer-helix positions *2o10* and *4o10* are far from the pore, corresponding cysteine substitutions were blocked by MTSET. Here we created the Kv1.2-based model of CaV2.1 using the above alignments. In this model, engineered cysteines in positions *i22* are surrounded by large hydrophobic residues, which would preclude cysteine ionization and hence reaction with MTSET. We further created CaV2.1 models with MTSET-substitutions in other positions and used Monte Carlo-energy minimizations to find energetically optimal conformations. The ammonium group of MTSET in positions *2i18* and *4i18* occludes the inner pore, while in positions *1i18* and *3i18* it protrudes in the domain interface. The ammonium group of MTSET in positions *2o10* and *4o10* approaches the pore, being closer to the pore axis than that in positions *1i18* and *3i18*. Thus, our model reinterprets experiments of Zhen et al. (2005), validates the above alignments, and suggests a similar folding of voltage-gated potassium and calcium channels. Supported by CIHR.

946-Pos Board B825

Modeling L-type Calcium Channel with Phenylalkylamines

Ricky C.K. Cheng[1], Denis B. Tikhonov[2], Boris S. Zhorov[1].
[1]McMaster University, Hamilton, ON, Canada, [2]Russian Academy of Sciences, St. Petersburg, Russian Federation.

Phenylalkylamines (PAAs), a major class of L-type calcium channel (LCC) blockers, have aromatic rings A and B connected by a flexible chain with cyano and ammonium groups proximal to rings A and B, respectively. Structural aspects of ligand-channel interactions remain unclear. We have built LCC models as in (Tikhonov and Zhorov, 2008) with KvAP, MthK, Kv1.2 and KcsA as templates and used Monte Carlo energy-minimizations to dock devapamil, verapamil, and gallopamil, which have three, four, and five methoxy groups, respectively. The PAA-LCC models have the following common features: meta-methoxy group in ring A accepts an H-bond from Y1179(3i10) in domain 3 inner-helix position 10, the ammonium group is stabilized at the focus of P-helices, and the cyano group coordinates a Ca2+ ion bound to the selectivity-filter glutamates in domains 3 and 4. The latter feature can explain the well-known effect of Ca2+ potentiation of PAA action. Our models are also consistent with structure-activity and mutational studies. For instance, mutation of Y1490(4i11) affects action of devapamil, but not verapamil and gallopamil (Johnson et al., 1996). In our models, the single meta-methoxy group in ring B of devapamil accepts an H-bond from Y1490(4i11), while meta- and para-methoxy groups in ring B of verapamil and gallopamil chelate the Ca2+ ion. Mutation T1066(3o14)Y in domain 3 outer-helix position 14 enhances action of devapamil and verapamil, but not gallopamil (Huber et al., 2004). Our models predict that para-methoxy group in ring A of devapamil and verapamil accepts an H-bond from Y3o14, while tri-methoxylated ring A of gallopamil is too bulky to approach Y3o14. Docking of devapamil in different models shows that the Kv1.2 template is most consistent with the experimental data. The closed (KcsA-based) model has the same ligand-channel contacts, but with weaker interaction energy. Supported by CIHR.

947-Pos Board B826

Effect Of $Ca_V\beta$ Subunits On Structural Organization Of $Ca_V1.2$ Calcium Channels As Revealed By Three-color Fret Microscopy

Evgeny Kobrinsky, Parwiz Abrahimi, Sam Thomas, JoBeth Harry, Chirag Patel, QiZong Lao, Nikolai Soldatov.
National Institute on Aging, Baltimore, MD, USA.

Voltage-gated $Ca_v1.2$ calcium channels play a crucial role in Ca^{2+} signaling. The poreforming α_{1C} subunit is regulated by accessory $Ca_v\beta$ and $\alpha_2\delta$ subunits. $Ca_v\beta$'s are cytoplasmic proteins of various size encoded by four different genes ($Ca_v\beta_1$ - β_4). Here we investigated the effect of three major $Ca_v\beta$ types, β_{1b}, β_{2d} and β_3, on the structure of $Ca_v1.2$ by measuring inter and intramolecular distances between α_{1C} and β in the plasma membrane of COS1 cells using three-color FRET microscopy. The results show that $Ca_v1.2$ channels are in close proximity in the plasma membrane. The presence of different $Ca_v\beta$'s does not result in significant differences in intramolecular distance between the termini of α_{1C}, but significantly affects intermolecular distance between the termini of neighbor α_{1C} subunits, which varies from 67 Å (β_{1b}) to 79 Å (β_3). Thus, our results show conclusively that plasma-membrane density of $Ca_v1.2$ channels depends on the type of $Ca_v\beta$'s present, suggesting a possible mechanism contributing to differences in Ca^{2+} signaling between various cell types.

948-Pos Board B827

Quantification Of L-type Ca Current Inactivation Mechanisms In Trout Ventricular Myocytes.

Laurent Salle[1], Caroline Cros[2], Daniel E. Warren[2], Holly A. Shiels[2], **Fabien Brette**[2].
[1]Universite de Caen, Caen, France, [2]University of Manchester, Manchester, United Kingdom.

Inactivation of L-type calcium current (I_{Ca}) is due to two mechanisms: voltage-dependent inactivation (VDI) and calcium-dependent inactivation (CDI). In fish cardiac myocytes, it is unknown whether Ca release from the sarcoplasmic reticulum (SR) participates in CDI of I_{Ca}. This study assesses the relative contribution of different inactivation mechanisms of I_{Ca} in trout ventricular myocytes. Trout ventricular myocytes were enzymatically isolated. I_{Ca} was recorded using whole cell patch clamp with Na- and K-free solutions to avoid contaminating currents. With a low concentration of a slow Ca buffer (EGTA 2mM) in the pipette solution, I_{Ca} inactivated slowly (compared to mammalian cardiac myocytes): the time to reach 37% of peak current (T_{37}) was 26.2 ± 2.4 ms (mean $\pm$ SEM, n=14). When a fast Ca buffer (BAPTA 10 mM) was present in the pipette solution I_{Ca} decay was similar to the decay in the presence of EGTA (T_{37}: 25.4 ± 1.5 ms, NS, t-test, n=9). When barium was used as a charge carrier, I_{Ba} inactivates mainly via VDI and T_{37} was significantly increased (43.7 ± 3.1 ms, n=9, $p<0.05$, t-test), albeit T_{37} is twice faster than in mammalian cardiac myocytes. We quantified the relative contribution of VDI and CDI according to the method previously described [Brette *et al.* (2004). *Circ Res;* **95;** e1-7]. We measured the fraction of current remaining 20 ms after its peak (I_{R20}). I_{R20} was 0.39 ± 0.03 in EGTA, 0.42 ± 0.02 in BAPTA and 0.64 ± 0.03 in barium. We estimated that CDI represents ~39% of total fast I_{Ca} inactivation, and that SR Ca release causes only ~12% of CDI. We conclude that the main inactivation mechanisms in the trout myocyte are due to VDI and CDI from Ca entering the cell via I_{Ca} and not SR Ca release. *Supported by the Wellcome Trust and the BBSRC.*

949-Pos Board B828

Egg Coat Proteins Activate Ca^{2+} Entry into Mouse Sperm via CATSPER Channels

Jingsheng Xia, Dejian Ren.
University of Pennsylvania, Philaselphia, PA, USA.

During mammalian fertilization, the contact between sperm and egg triggers increases in intracellular Ca^{2+} concentrations ($[Ca^{2+}]_i$) in sperm. Voltage-gated Ca^{2+} channels (Ca_Vs) are believed to mediate the initial phase of $[Ca^{2+}]_i$ increases in sperm induced by egg coat (zona pellucida, ZP) glycoproteins, while

the sustained phase is believed to be mediated via store depletion-activated Ca^{2+} entry. Using patch-clamp recording and Ca^{2+} imaging, we show here that Ca_V channel currents, while found in spermatogenic cells, are not detectable in epididymal sperm and are not essential for the ZP-induced $[Ca^{2+}]_i$ changes. Instead, CATSPER channels localized in the distal portion of sperm (the principal piece) are required for the ZP-induced $[Ca^{2+}]_i$ changes. Furthermore, the ZP-induced $[Ca^{2+}]_i$ increase starts from the sperm tail and propagates toward the head.

Voltage-gated Ca Channels II

950-Pos Board B829

A Simple Link Between Gating And Pore Occupancy Can Describe Complex Ion-Dependent Kinetics Of Ca^{2+} Channels

Roman Shirokov, Anna Angelova, Alexandra Uliyanova.
New Jersey Medical School - UMDNJ, Newark, NJ, USA.

Several aspects of Ca^{2+} channel gating depend on permeant ions. These effects are difficult to describe in terms of regular ''states-and-rates'' models, which suggest that the channel does not change kinetic state(s) while it is open to pass current. We propose an approach to overcome this limitation. An open state is considered to have a minimum of two ''sub-states'': one is occupied by permeant ion and the other is not. The sub-states are allowed to have different kinetic paths of exit from the open state.

A minimalistic model of this sort explains the U-shaped voltage-dependence of inactivation by incorporating our previous finding that the apparent affinity of the channel pore for permeant ion increases during inactivation (Babich et al., JGP, 2007). The model implies that the tighter binding of permeant ions to the pore prevents current through inactivated channels, as if the pore is the ''inactivation gate''. This idea is in an apparent contradiction with the view that the mechanism of inactivation of Ca^{2+} currents, ''CDI'', is independent from that of Ba^{2+} currents, ''VDI'' (e.g., Barret and Tsien, PNAS, 2008). Here we show that our model describes well effects of molecular interventions that appear to differentially alter ''CDI'' and/or ''VDI''. Therefore, ion- and voltage-dependent components of inactivation may converge to act at the channel's pore.

951-Pos Board B830

Kinetic Modeling of CaV3.1

Katie C. Bittner[1], Lorin Milescu[2], Dorothy A. Hanck[1].
[1]University of Chicago, Chicago, IL, USA, [2]Harvard University, Boston, MA, USA.

T-type calcium channel kinetics have been well characterized at the macroscopic level, but less well so at the single channel level. The most thorough single channel kinetic analyses have been performed using recordings from native tissues where the specific isoform(s) present is unknown. As a result there is some discrepancy as to magnitude and voltage dependence of fundamental descriptors such as mean open time. It has been reported to be 0.5-2.5ms and either weakly voltage dependent or voltage independent (summarized in Perez-Reyes 2003). Macroscopic current measurements, on the other hand, are consistent with a voltage dependent O->C transition, suggesting that mean open time is voltage dependent. Bandwidth differences and other issues associated with signal to noise ratio for these conductance channels have no doubt contributed to measured durations. The development of gating models for these channels has been hampered by the paucity of high quality single channel data. Furthermore, previously published gating models of $Ca_V3.1$ correctly approximate the voltage dependence and time course of the macroscopic currents of $Ca_V3.1$ but fail to appropriately recapitulate the gating currents (Serrano et al 1999, Burgess et al 2002). We have utilized low noise recording methods to obtain higher bandwidth single channel data and paired it with maximum idealized point-likelihood analysis in QuB to estimate rate constants and their voltage dependence from single channel data for inclusion in developing models that correctly recapitulate macroscopic, single channel, and gating current data. Supported by F31-NS058334 (K.B.) and RO1-HL065680 (D.H.)

952-Pos Board B831

Voltage-sensor Pharmacology Of Voltage-activated Calcium Channels (cav)

Mirela Milescu, Kenton J. Swartz.
NIH/NINDS, Bethesda, MD, USA.

The four voltage sensors in Cav channels have distinct amino acid sequences, raising fundamental questions about their relative contributions to the function and regulation of the channel. Studies of Kv channels identified a S3b-S4 helix-turn-helix motif, termed paddle motif, which moves at the protein-lipid interface interface to drive activation of the voltage-sensors. This motif is an important pharmacological target for amphipathic neurotoxins and it has been suggested that is conserved in Cav and other voltage-gated ion channels. Here we show that the four S3b-S4 paddle motifs within the Cav channel could be transplanted into four-fold symmetric Kv channel to individually examine their contributions to the kinetics of voltage sensor activation and regulation by toxins.

953-Pos Board B832

Independent Contributions Of Segments IS6 And IIS6 To Activation Gating Of $Ca_V1.2$

Michaela Kudrnac[1], Stanislav Beyl[1], Annette Hohaus[1], Anna Stary[2], Thomas Peterbauer[1], Eugen Timin[1], **Steffen Hering**[1].
[1]Pharmacology and Toxicology, Vienna, Austria, [2]Institute for Theoretical Chemistry, Vienna, Austria.

Voltage dependence and kinetics of activation of $Ca_V1.2$ channels are affected by structural changes in pore lining S6 segments of the α_1-subunit. Significant effects on channel activation are induced by either proline or threonine substitutions in the lower third of segment IIS6 ('bundle crossing region'). Here we report that S435P in IS6 results in a large shift of the activation (−26mV) curve and slowed current kinetics. Threonine substitutions in positions Leu429 and Leu434 induced a similar kinetic phenotype with shifted activation curves.

Double mutations in segments IS6 and IIS6 induced additive shifts of the activation curves, e.g.: L429T/I781T (-44.0 ± 1.0), L434T/I781T (-50.3 ± 0.8), L429T/L779T (-22.5 ± 0.8) and L434T/L779T (-32.3 ± 0.8). If the gating sensitive residues in the two neighboring segments IS6 and IIS6 do not interact then the change in free energy (ΔG_{double}) of the double mutant is equal to the sum of the changes in free energy of the two single mutations ($\Delta G_{mut\ IS6}$ and $\Delta G_{mut\ IIS6}$ see scheme, see also Horovitz 1996). Double mutant cycle analysis revealed that the studied IS6 and IIS6 mutations are energetically independent and thus have independent impacts on activation gating.

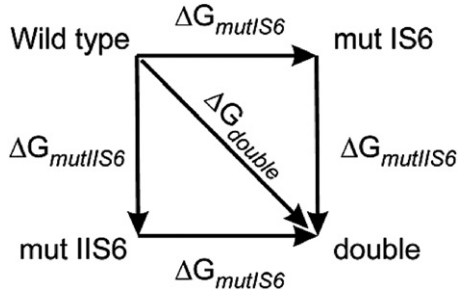

Supported by FWF-Project P19614-B11.

954-Pos Board B833

Role of S4 segments in Ca_v1 and Ca_v3 channels: gating and current density

Juan F. Higueldo-Garcia, Jonatan Barrera-Chimal, Juan C. Gomora.
Institute of Cell Physiology, UNAM, Mexico City, Mexico.

Gating of voltage-dependent calcium channels (Ca_v) is determined by S4 segments in each of the four α1-subunit domain's. In the S4 segments, also known as voltage sensors, every third position there is a positive charged residue (lysine or arginine). However, both high-voltage (HVA) and low-voltage (LVA or T-type) activated Ca_v channels, show S4 segments with very similar sequences. This issue had already been investigated in some members of T-type Ca_v3 family, mainly in $Ca_v3.1$ (α1G), and one report on $Ca_v3.2$ (α1H), but there is no data on the $Ca_v3.3$ (α1I). To investigate the role of S4 segments in the differences in gating between $Ca_v3.3$ and $Ca_v1.2$ we made a chimerical approach swapping the S4 segment of domain II of $Ca_v3.3$ with the corresponding S4 segment of $Ca_v1.2$. We have used HEK-293 cells and the whole-cell patch clamp technique to characterize the functional expression of the constructs. Our preliminary results indicate that the substitution of the IIS4 segment of $Ca_v3.3$ for that of $Ca_v1.2$ induce a 25 mV positive shift in the *I-V* peak with respect to the $Ca_v3.3$ wild type (WT). Also, the Boltzmann parameters were significantly different between the WT and the chimeric channel *I-V* curves. There was no appreciable change in the kinetics of the currents. An unexpected result was a drastic decrease (< 95%) in the current density of the chimeric channel. A possible explanation is that the IIS4 (the whole or some residues of it) of $Ca_v1.2$ is interacting with the rest of the channel protein in such way that makes more stable the closed state of the channel. Additional experiments are under way to further study this observation.

This work was supported by CONACYT México J50250Q.

955-Pos Board B834

Depolarization-induced Potentiation Of Cav1.1 Does Not Require The Distal C-terminus

Joshua D. Ohrtman, Kurt G. Beam.
University of Colorado Health Sciences Center, Denver, CO, USA.

In adult skeletal muscle, the majority of the L-type Ca^{2+} channel CaV1.1 subunit is truncated post-translationally at residue 1664 (PNAS, 102:5274-79), raising the question of the functional role of the distal residues (1665-1873). It has been suggested (J Neurosci.17:1243-55; J Biol Chem. 277:4079-87) that (i) the distal C-terminus is non-covalently associated with the remainder of the channel, (ii) reduces channel open probability, and (iii) loses this inhibitory effect as a result of phosphorylation during strong depolarization. In regard to point (ii), previous analysis of L-type ionic conductance (G) and